

Partially suppressed long-range order in the Bose-Einstein condensation of polaritons

D. Sarchi* and V. Savona

Institute of Theoretical Physics, Ecole Polytechnique Fédérale de Lausanne EPFL, CH-1015 Lausanne, Switzerland

(Dated: September 27, 2018)

We adopt a kinetic theory of polariton non-equilibrium Bose-Einstein condensation, to describe the formation of off-diagonal long-range order. The theory accounts properly for the dominant role of quantum fluctuations in the condensate. In realistic situations with optical excitation at high energy, it predicts a significant depletion of the condensate caused by long-wavelength fluctuations. As a consequence, the one-body density matrix in space displays a partially suppressed long-range order and a pronounced dependence on the finite size of the system.

PACS numbers: 71.36.+c, 71.35.Lk, 42.65.-k, 03.75.Nt

I. INTRODUCTION

Bose-Einstein condensation (BEC) is one of the most remarkable manifestations of quantum mechanics at the macroscopic scale.¹ The key feature of BEC of an interacting Bose gas is the formation of off-diagonal long range order (ODLRO),^{2,3} i.e. the fact that the spatial correlation $g^{(1)}(\mathbf{r}, \mathbf{r}') = n(\mathbf{r}, \mathbf{r}') / \sqrt{n(\mathbf{r})n(\mathbf{r}')}$ (where $n(\mathbf{r}, \mathbf{r}')$ is the one-body density matrix, while $n(\mathbf{r})$ is the particle density) extends over the whole system size. The BEC mechanism is the key to understand superconductivity and superfluidity,¹ and was the object of renewed interest following its recent discovery in diluted alkali atoms.⁴ Another candidate system for the observation of BEC is that of excitons⁵ or exciton-polaritons⁶ in insulating crystals. Recently, in particular, many theoretical^{7,8,9,10} and experimental^{11,12,13,14} efforts have been devoted to BEC of microcavity polaritons. Due to the strong mutual polariton interactions, the system is expected to deviate significantly from the ideal Bose gas picture. Interactions are responsible of quantum fluctuations, namely of the emergence of collective eigenmodes that differ from the single-particle states.⁴ Quantum fluctuations in the polariton gas are expected to be more relevant than in a diluted atomic gas. This will lead to a depletion of the condensate that can be very important, reminding of the prototypical case of ⁴He in which a condensate fraction of less than 10% at equilibrium is achieved. Deviations from thermal equilibrium might still enhance this tendency. As an example, theoretical predictions for bulk polaritons suggest that an initial condensate population can be totally depleted by quantum fluctuations within a sufficiently long time¹⁵. In the present case, a full depletion is only prevented by the short polariton lifetime, allowing to a considerable fraction of the particles in the condensate to undergo radiative recombination before scattering to the excited states. Another indication of the importance of quantum fluctuations comes from the measurement¹¹ of the second-order time-correlation function at zero delay $g^{(2)}(0)$. There, quantum fluctuations might explain the large deviation from the quantum limit ($g^{(2)}(0) = 1$), observed far above the condensation threshold. The role played by quantum fluctuations is even more important

in the light of the two-dimensional nature of microcavity polaritons. For a two-dimensional system in the thermodynamic limit, as stated by the Hohenberg-Mermin-Wagner theorem,¹⁶ the long-wavelength fluctuations diverge, and ODLRO cannot arise. However condensation is prohibited only in infinitely extended systems. Realistic polariton systems, based both on III-V¹⁷ and on II-VI¹³ semiconductors, exhibit disorder that tends to localize the lowest polariton levels over a few tens of μm ¹⁷. In these situations, it was rigorously proved that the discrete energy spectrum, arising either from quantum confinement in a finite system¹⁸ or from disorder induced polariton localization,¹⁹ allows condensation in a thermal equilibrium situation, although the occurrence of ODLRO could be inhibited, depending on the localization length and on the disorder amplitude.¹⁹ Very recently, a direct measurement of the spatial correlation function in a II-VI semiconductor based microcavity¹⁴, provided a striking experimental signature of polariton condensation with formation of ODLRO.

In order to experimentally assess polariton BEC, it is important to predict how ODLRO manifests itself in a non-equilibrium situation, in a localized geometry, and in presence of quantum fluctuations. To this purpose, a field-theoretical approach is required for a proper description of the relaxation kinetics and of the quantum fluctuations in presence of mutual interaction.

In this work we develop a kinetic theory of polaritons subject to mutual interaction, in which the field dynamics of collective excitations is treated self-consistently along with the condensation kinetics. We start from a number-conserving Bogolubov approach^{20,21} that describes the collective modes of a Bose gas properly accounting for the number of particles in the condensate. This is required in order to develop kinetic equations for the description of condensate formation. We then derive a hierarchy of density matrix equations, including polariton-phonon scattering via deformation-potential interaction and exciton-exciton scattering in the exciton-like part of the lower-polariton branch. This latter mechanism is based on the model recently developed by Porrás *et al.*²². The hierarchy is truncated to include coupled equations for the populations in the lower polariton branch and for the two-particle correlations between the condensate

and the excitations. For the truncation, we assume that higher-order correlations evolve much faster than the relaxation dynamics. The kinetic equations obtained in this way are solved numerically, assuming a steady-state pump at high energy within the exciton-like part of the polariton branch. The solution is carried out by accounting self-consistently for the density-dependent Bogolubov spectrum of the collective excitations of the polariton gas. We show how this model predicts a dominant effect of quantum fluctuations that result in a significant condensate depletion under typical excitation conditions. In particular, we discuss the role of quantum confinement in a system of finite size and show how ODLRO manifest itself in typical experimental conditions. Our results provide a clear explanation of the partial suppression of ODLRO that characterizes the experimental findings¹⁴.

The paper is organized as follows. In Section II we describe in detail the theoretical framework of the present analysis. Section III is devoted to the presentation of the numerical solution of the kinetic equations and to the discussion of the results in the light of recent polariton BEC experiments. In Section IV we present our conclusions.

II. THEORY

We consider the polariton in the lower branch of the dispersion as a quasi-particle in two dimensions,²³ described by the Bose field \hat{p}_k , obeying $[\hat{p}_k, \hat{p}_{k'}^\dagger] = \delta_{kk'}$. The lower polariton Hamiltonian in presence of Coulomb and polariton-phonon scattering is²⁴

$$H = H_0 + \frac{1}{2} \sum_{kk'q} v_{kk'}^{(q)} \hat{p}_{k+q}^\dagger \hat{p}_{k'-q}^\dagger \hat{p}_{k'} \hat{p}_k + \sum_{kk'q} g_{kk'}^{(q)} (b_q^\dagger + b_{-q}) (\hat{p}_k^\dagger \hat{p}_{k'} + \hat{p}_{k'}^\dagger \hat{p}_k), \quad (1)$$

where $H_0 = \sum_k \hbar\omega_k \hat{p}_k^\dagger \hat{p}_k + \sum_q \hbar\omega_q b_q^\dagger b_q$ is the free Hamiltonian for polaritons and phonons. The quantity $v_{kk'}^{(q)}$ arises from the Coulomb interaction between excitons v_{XX} and from the oscillator strength saturation due to Pauli exclusion v_{sat} ^{25,26,27}, as

$$v_{kk'}^{(q)} = v_{XX} X_{k+q} X_{k'-q} X_k X_{k'} + v_{sat} X_{k'-q} (C_{k+q} X_k + X_{k+q} C_k) X_{k'}. \quad (2)$$

Here the X_k, C_k are the Hopfield coefficients representing the excitonic and the photonic weights respectively, in the lower polariton field, i.e. $\hat{p}_k = X_k \hat{B}_k + C_k \hat{A}_k$. Here \hat{B}_k and \hat{A}_k are the exciton and the photon destruction operators respectively²⁴. In Eq.(2) we consider the interaction matrix elements in the small-momentum limit (consistently with the restriction of the analysis to the lower polariton branch of the dispersion)^{9,22,25}, i.e.

$$v_{XX} = \frac{6E_b a_0^2}{A} \\ v_{sat} = -\frac{\hbar\Omega_R}{n_{sat} A}, \quad (3)$$

where E_b is the exciton binding energy, a_0 is the exciton Bohr radius, $2\hbar\Omega_R$ is the microcavity vacuum-field Rabi splitting, $n_{sat} = 7/16\pi a_0^2$ is the exciton saturation density^{25,28} and A is the system quantization area. The quantity $g_{kk'}^{(q)}$ describes the deformation potential interaction of polaritons with acoustic phonons^{9,29} and reads

$$g_{kk'}^{(q)} = i\sqrt{\frac{\hbar|q|}{2\rho AL_z u}} X_k X_{k'} \times [a_e I_e^{\parallel}(|q|) I_e^{\perp}(q_z) - a_h I_h^{\parallel}(|q|) I_h^{\perp}(q_z)]. \quad (4)$$

Here, ρ and u are the density and the longitudinal sound velocity in the semiconductor, respectively, L_z is the quantum well width and $a_{e(h)}$ are the electron(hole) deformation potentials. The terms $I_{e(h)}^{\parallel}(|q|)$ and $I_{e(h)}^{\perp}(q_z)$ are the superposition integrals of the exciton envelope function with the phonon wave function (plane wave) in the in-plane and z -directions, respectively, and read

$$I_{e(h)}^{\parallel}(|q|) = [1 + (a_0 q_z m_{e(h)})/2(m_e + m_h)]^{-3/2} \\ I_{e(h)}^{\perp}(q_z) = \int dz |f_{e(h)}(z)|^2 e^{iq_z z}, \quad (5)$$

where $m_{e(h)}$ is the electron (hole) mass while $f_{e(h)}(z)$ are the electron(hole) envelope functions in the growth direction, according to the exciton envelope function picture³⁰.

For a kinetic description, a number-conserving approach^{20,21} is required. This formalism allows treating in a self-consistent way the field dynamics and the population kinetics, and describes correctly the condensate in- and out-scattering rates. In the number-conserving approach, the polariton field is expressed as

$$\hat{p}_k = P_k \hat{a} + \tilde{p}_k, \quad (6)$$

i.e. the sum of a condensate operator $P_k \hat{a}$ and a single-particle excitation operator \tilde{p}_k .²⁰ The condensate operator obeys Bose commutation rules $[\hat{a}, \hat{a}^\dagger] = 1$. The quantity $N_c = \langle \hat{a}^\dagger \hat{a} \rangle$ is the population of condensed particles, while P_k represents the condensate wave function in momentum space. The single-particle excitation field \tilde{p}_k is orthogonal to the wave function of the condensate, i.e. $\sum_k P_k^* \tilde{p}_k = 0$, and obeys the modified Bose commutation rule $[\tilde{p}_k, \tilde{p}_{k'}^\dagger] = \delta_{kk'} - P_k P_{k'}^*$. Using these definitions, the total population at momentum k is $N_k = \langle \hat{p}_k^\dagger \hat{p}_k \rangle = |P_k|^2 N_c + \tilde{N}_k$, where $\tilde{N}_k = \langle \tilde{p}_k^\dagger \tilde{p}_k \rangle$ is the population of non-condensed particles. Within the number conserving approach, a quantum fluctuation is defined by the operator²⁰

$$\hat{\Lambda}_k^\dagger \equiv \frac{1}{\sqrt{N}} \hat{a} \tilde{p}_k^\dagger \quad (7)$$

that promotes a particle from the condensate to the excited states. N is the total number of particles. This field can be formally written via a Bogolubov transformation as $\hat{\Lambda}_k = U_k \hat{\alpha}_k + V_{-k}^* \hat{\alpha}_{-k}^\dagger$, where U_k and V_{-k}^* are

modal functions, and \hat{a}_k are Bose operator describing the collective excitations at energy E_k .^{4,20}

Our model is based on two key-assumptions. First, we separate the single-particle energy spectrum into a lower energy coherent part and an incoherent part at higher energies. This is depicted in Fig. 1 (a) for the typical energy-momentum dispersion of the lower polariton branch. In a condensate, collective Bogolubov excitations affect mostly the lower-energy part of the spectrum. As the energy becomes larger than the total interaction energy vN_c (where v is a measure of the interaction matrix element), $U_k \rightarrow 1$ and $V_k \rightarrow 0$, and the collective modes thus approach the single-particle states. Hence, it is mostly in the low-energy region that quantum fluctuations will affect the condensate kinetics. A customary³¹ approximation consists in restricting the quantum kinetic treatment to the coherent region, while the dynamics within the incoherent region is modeled in terms of a simple Boltzmann population kinetics.

The separation, for the lower polariton branch, naturally coincides with that between the strong-coupling region and the flat exciton-like part of the dispersion, as illustrated in Fig. 1(a). The second approximation is made possible by the remark that, given the large Coulomb scattering amplitude, the field dynamics of collective Bogolubov excitations takes place much faster than energy relaxation mechanisms, made slow by the steep polariton energy-momentum dispersion that reduces the space of final states available for scattering processes. We thus assume that, on the timescale of the relaxation, a quasi-stationary spectrum of collective Bogolubov excitations arises, that evolves adiabatically and is computed self-consistently at each time step in the kinetics, by means of the Popov version of the Hartree-Fock-Bogolubov approximation (HFB Popov). This approximation is justified by the two following arguments. First, in equilibrium conditions, it is known that the HFB Popov approximation predicts collective excitations in excellent agreement with the measured excitation spectra of a weakly interacting Bose gas, when the temperature is sufficiently low, i.e. $T \leq 0.5T_c$, where T_c is the critical temperature. Alternatively, this condition corresponds to a density considerably above the critical density.^{32,33} Second, our present purpose is not to determine the exact spectrum of the collective multipole oscillations of the polariton gas close to the condensation threshold. It is rather to estimate how the density-dependent changes in the spectrum affect the relaxation dynamics and the coherent scattering processes significantly above the condensation threshold, when ODLRO becomes detectable. In addition, close to threshold, the polariton relaxation dynamics and the coherent scattering processes are expected to be only marginally affected by the details of the spectrum, because the populations in the condensate and in the low-lying excited states are small, as argued in Ref. 22.

The kinetics is described in terms of a density-matrix hierarchy whose time-evolution is obtained from the

Heisenberg equations of motion. Coulomb interaction terms within the incoherent region are treated consistently with the Boltzmann picture, as was done by Porras *et al.*²². In particular, we assume that, in the incoherent region, the population of the exciton-like polaritons is thermally distributed with an effective temperature defined by $k_B T_x \equiv e_x/n_x$, where k_B is the Boltzmann constant, n_x is the total particle density and e_x is the total energy density in the incoherent region (as shown below, these two quantities are determined self-consistently during relaxation, via Boltzmann equations). Within this picture, the processes of two particles in the incoherent region scattering into one particle in the incoherent region and one in the coherent region, result in an effective energy relaxation mechanism towards the bottom of the polariton branch. In the coherent region, on the other

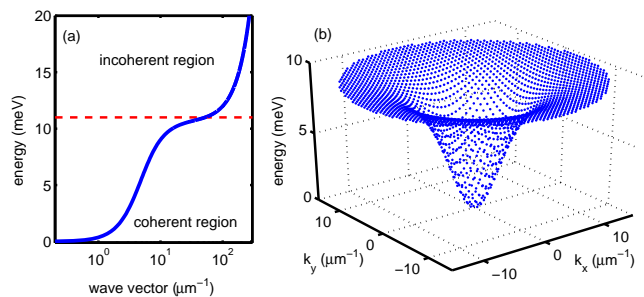


FIG. 1: (a) Energy-momentum lower-polariton dispersion. Notice the logarithmic horizontal scale. (b) Energy-momentum plot of the discrete lower-polariton states in the coherent region, as used in the simulations for $A = 100 \mu\text{m}^2$.

hand, we extend the hierarchy of equations to the next order, thus including two-body (four operator) correlations. The most important of these two-body correlations entering our equations describes coherent processes where two polaritons are scattered between the condensate and the excited states within the coherent region. It is given by $\tilde{m}_k = N\langle \hat{\Lambda}_k \hat{\Lambda}_{-k} \rangle$ and describes the main effect of quantum fluctuations. These processes do not conserve energy and could not be described in terms of Boltzmann equations for the populations of the single-particle states. They are made possible only because, in a condensed system, the actual eigenstates $\{|\nu\rangle\}$ are collective modes and differ from the single-particle states $\{|k\rangle\}$. As a consequence, the quantities $\langle \nu | \hat{\Lambda}_k \hat{\Lambda}_{-k} | \nu \rangle$ are finite. As already pointed out, their amplitude is expected to decrease for increasing energy E_k . We have checked that our model reproduces this behaviour, as is reported below in connection with Fig. 4. This proves that our approximation, consisting in the separation into two energy regions, is consistent with the real behaviour of the system. A full treatment in terms of quantum kinetics is made here prohibitive by the inclusion of a very large number of states in the exciton-like part of the dispersion, that is needed in order to model the initial high-energy excitation used in photoluminescence ex-

periments. Models assuming an initial population in the lower-energy part of the spectrum¹⁵, can instead treat the full spectrum consistently. In fact, in that case, the only relevant coherent scattering processes involve states with energy smaller than the interaction energy vN (where v is the interaction matrix element and N is the initial condensate population, see e.g. Fig. 3 of Ref. 15).

The polariton-phonon scattering is treated within a shifted-pole Markov approximation, resulting in standard Boltzmann contributions²⁹. For the calculations, we assume a finite-size homogeneous system of square shape and area A with periodic boundary conditions, resulting in spatially a uniform condensate wave function, i.e. $P_k = e^{i\phi} \delta_{k,0}$.³⁴ In a realistic condensate, this assumption is valid everywhere, except within a distance from the boundary equal to the healing length $\xi = \hbar/\sqrt{Mv n^4}$. For polaritons, we find $\xi \approx 1 \mu\text{m}$ for the estimated density threshold. The confinement can model both finite size polariton traps³⁵ and the situation close to a local minimum of the disorder potential in extended systems.^{13,17} The finite size results in quantum confinement and thus in a discrete energy spectrum, with a gap between ground and first excited state $\Delta = \hbar^2(2\pi)^2/(M_{pol}A)$.⁹

Within these prescriptions (see Appendix) the kinetic equations are:

$$\begin{aligned}
\dot{N}_c &= -\gamma_0 N_c + \dot{N}_c|_{ph} + \dot{N}_c|_{XX} + \frac{2}{\hbar} \sum_k v_{k,-k}^{(k)} \text{Im}\{\tilde{m}_k\} \\
\dot{\tilde{N}}_k &= -\gamma_k \tilde{N}_k + \dot{\tilde{N}}_k|_{ph} + \dot{\tilde{N}}_k|_{XX} - \frac{2}{\hbar} v_{k,-k}^{(k)} \text{Im}\{\tilde{m}_k\} \\
\dot{\tilde{m}}_k &= -2 \left[\gamma_0 + i\omega_k + \frac{i}{\hbar} v_{k,0}^{(0)} (N_c - \tilde{N}_k - 5/2) \right] \tilde{m}_k \\
&\quad - \frac{i}{\hbar} \left[\sum_q v_{q,-q}^{(k-q)} \tilde{m}_q - 2v_{k,-k}^{(k)} N_c (N_c - 1) \right] (1 + 2\tilde{N}_k) \\
&\quad + 2 \frac{i}{\hbar} (1 + 2N_c) \sum_q v_{q,-q}^{(q)} \langle \tilde{p}_q^\dagger \tilde{p}_{-q}^\dagger \tilde{p}_k \tilde{p}_{-k} \rangle \\
\dot{n}_x &= -\gamma_x n_x + \dot{n}_x|_{ph} + \dot{n}_x|_{XX} + f.
\end{aligned} \tag{8}$$

The $\gamma_k = \gamma_c |C_k|^2$ is the polariton radiative lifetime, $|C_k|^2$ being the photon fraction in the polariton state, γ_c the cavity photon lifetime, and γ_x the exciton lifetime. The quantity f denotes the pump intensity producing a population in the incoherent region. The suffixes “ ph ” and “ XX ” denote the Boltzmann scattering terms for polariton-phonon scattering²⁹ and for exciton-exciton scattering in the incoherent region²².

In the equation for \tilde{m}_k some simplifications were introduced. First, we have fully neglected the contributions due to both energy relaxation mechanisms. This is consistent with our adiabatic assumption, as the dynamics of the correlation \tilde{m}_k reflects the time-evolution of collective excitations, taking place on a much faster timescale than relaxation. Second, the higher order three-body correlations, arising as the next level of the correlation hierarchy, have been factored into products of one- and two-body correlations. Furthermore, we

assume the identity $\langle \hat{a}^\dagger \hat{a}^\dagger \hat{a} \hat{a} \rangle = N_c(N_c - 1)$ to hold, as expected for a macroscopic condensate occupation, $N_c \gg 1$. Third, always according to the adiabatic approximation, the two-body correlation function *between* condensate excitations, $\langle \tilde{p}_q^\dagger \tilde{p}_{-q}^\dagger \tilde{p}_k \tilde{p}_{-k} \rangle$ is evaluated in a quasi-stationary limit. It can thus be expressed in terms of the modal functions U_k and V_{-k}^* obtained by diagonalizing the stationary Bogolubov problem at each time step in the kinetics. Starting from the dynamical equation $\dot{\hat{\Lambda}}_k = (\omega_k + v_{k,0}^{(0)} \xi_k) \hat{\Lambda}_k + v_{k,k}^{(k)} \xi_k \hat{\Lambda}_k^\dagger$, with $\xi_k = (N_c - \tilde{N}_k)/N$, we derive the actual eigenvalues $E_k = [(\omega_k + v_{k,0}^{(0)} \xi_k)^2 - (v_{k,k}^{(k)} \xi_k)^2]^{1/2}$, while the modal functions are given by

$$|V_k|^2 = \xi_k \frac{[E_k - (\omega_k + v_{k,0}^{(0)} \xi_k)]^2}{(v_{k,k}^{(k)} \xi_k)^2 - [E_k - (\omega_k + v_{k,0}^{(0)} \xi_k)]^2} \tag{9}$$

and the normalization $|U_k|^2 - |V_k|^2 = \xi_k$. In this limit (see Appendix) we can replace in (8) the following expression

$$\begin{aligned}
\langle \tilde{p}_q^\dagger \tilde{p}_{-q}^\dagger \tilde{p}_k \tilde{p}_{-k} \rangle &\simeq \Upsilon(N) \left[\left| \sum_k U_k V_k^* (1 + 2\tilde{N}_k) \right|^2 \right. \\
&\quad \left. + \sum_k 2\chi_k \tilde{N}_k \left(\chi_k \tilde{N}_k + 2|V_k|^2 \right) + 2|V_k|^4 \right],
\end{aligned} \tag{10}$$

where $\Upsilon(N) = N^2[(N_c + 1)(N_c + 2)]^{-1}$ and $\chi_k = \xi_k + 2|V_k|^2$. $\tilde{N}_k = \langle \hat{a}_k^\dagger \hat{a}_k \rangle$ is the population of the Bogolubov modes, which can be expressed in terms of the single-particle population via the exact relation $\tilde{N}_k = (N/(N_c + 1)) \times [(|U_k|^2 + |V_k|^2)\tilde{N}_k + |V_k|^2]$. This finally brings to a closed set of kinetic equations for the amplitudes \tilde{m}_k , the populations N_c , \tilde{N}_k , and the total density n_x in the incoherent region.

Before discussing the numerical solution of Eqs. (8), we present the detailed expressions of the Boltzmann terms entering these equations. Their expressions are formally identical to the corresponding terms derived in Ref. 9 (for polariton-phonon scattering) and in Ref. 22 (for exciton-exciton scattering), with an important difference: in the present case, the actual HFB Popov spectrum E_k replaces the non-interacting single-particle spectrum. Here we report the expressions of these terms, the details of the derivation being described in Refs.^{9,22}.

$$\begin{aligned}
\dot{N}_k|_{ph} &= A \left[W_{x \rightarrow k}^{ph} n_x (1 + N_k) - W_{k \rightarrow x}^{ph} N_k \left(\eta + \frac{N_{k'}}{A} \right) \right] + \\
&\quad + \sum_{k' \in U_{coh}} \left[W_{k' \rightarrow k}^{ph} N_{k'} (1 + N_k) + \right. \\
&\quad \left. - W_{k \rightarrow k'}^{ph} N_k (1 + N_{k'}) \right],
\end{aligned} \tag{11}$$

$$\dot{N}_k|_{XX} = W_{x \rightarrow k}^{XX} n_x^2 (1 + N_k) - W_{k \rightarrow x}^{XX} n_x N_k, \tag{12}$$

$$\dot{n}_x|_{ph} = \sum_{k \in U_{coh}} \left[W_{k \rightarrow x}^{ph} N_k (\eta + n_x) - W_{x \rightarrow k}^{ph} n_x (1 + N_k) \right] \quad (13)$$

and

$$\dot{n}_x|_{XX} = -\frac{1}{A} \sum_{k \in U_{coh}} \left[W_{x \rightarrow k}^{XX} n_x^2 (1 + N_k) - W_{k \rightarrow x}^{XX} n_x N_k \right], \quad (14)$$

where $\eta A \equiv [(m_e + m_h)k_B T_x] A / 2\pi \hbar^2$ is the number of states in the incoherent region, and U_{coh} denotes the coherent region. Here, $N_k = \tilde{N}_k$ for $k \neq 0$ and $N_0 = N_c$. Note that in Eqs. (11-14) we use the fact that $n_x/\eta \ll 1$ and $k \ll k_x$, where k_x is the averaged momentum of the exciton distribution in the incoherent region. The rates appearing in Eq. (11-14) are given by

$$W_{k \rightarrow k'}^{ph} = \frac{2L_z}{\hbar} \left| g_{k,k'}^{\bar{q}} \right|^2 \frac{|E_k - E_{k'}|}{(\hbar u)^2 q_z} \left[n_{kk'}^{ph} + \theta(E_k - E_{k'}) \right],$$

$$|\bar{q}| = \sqrt{|k - k'|^2 + \bar{q}_z^2} = |E_k - E_{k'}|/\hbar u, \quad (15)$$

where $n_{kk'}^{ph}$ is the population of phonons having energy $E = E_k - E_{k'}$;

$$W_{x \rightarrow k}^{XX} = \frac{2\pi}{\hbar k_B T_x} \left| v_{k_x, k_x}^{(k_x)} \right|^2 A^2 e^{(E_k - E_{k_x})/k_B T_x}, \quad (16)$$

$$W_{k \rightarrow x}^{XX} = \frac{(m_e + m_h)}{\hbar^3} \left| v_{k_x, k_x}^{(k_x)} \right|^2 A^2 e^{2(E_k - E_{k_x})/k_B T_x}. \quad (17)$$

In all these expressions, consistently with our assumption the spectrum in the incoherent region E_{k_x} is the single-particle spectrum, only accounting for the overall density-induced blue shift of the polariton branch. Besides the set of equations (8), the model is completed by the introduction of an equation describing the evolution of the energy density in the incoherent region e_x . Following the procedure of Ref. 22, this equation reads

$$\dot{e}_x = - \sum_{k \in U_{coh}} \frac{E_k}{A} \left[W_{x \rightarrow k}^{XX} n_x^2 (1 + \tilde{N}_k) - W_{k \rightarrow x}^{XX} n_x N_k \right] - \gamma_x (k_B T_x) n_x + (k_B T_L) f - w^{ph}. \quad (18)$$

Here, the first term represents the heating of the incoherent population, produced by the exciton-exciton scattering process and imposed by energy conservation; the second term is the cooling due to the exciton radiative recombination; the third term is originated by the assumption that the incoherent population is created at the lattice temperature T_L ; the fourth term represents the cooling induced by exciton-phonon coupling and it is evaluated as in Eq. (21) of Ref. 22.

III. NUMERICAL RESULTS

Numerical solutions assuming a steady state pump have been computed in the time domain. We assume

parameter values relative to the CdTe microcavity of Ref. 14, with Rabi splitting $2\hbar\Omega_R = 26$ meV and cavity photon-exciton detuning $\delta = 5$ meV, at the lattice temperature $T = 10$ K. The quantization area is assumed everywhere $A = 100 \mu\text{m}^2$, unless specified, consistent with estimates of polariton localization length,¹³ and gives rise to the discrete set of polariton states plotted in Fig. 1(b). For this system we obtain from Eq. (3) $v_{XX} = 3.3 \times 10^{-5}$ meV, $v_{sat} = -0.5 \times 10^{-5}$ meV and the resulting polariton-polariton interaction matrix element at zero momentum is $v_{0,0}^{(0)} = 6 \times 10^{-5}$ meV. The solutions always display steady-state long-time values after an initial transient, as shown in Fig. (2). Here we also notice that, during the early stages of the condensate growth, the scattering processes favor condensation, through the positive values taken by $\text{Im}\{\tilde{m}_k\}$. Immediately afterwards, when a large condensate population is reached, the quantity $\text{Im}\{\tilde{m}_k\}$ changes sign and coherent scattering terms start depleting the condensate. In

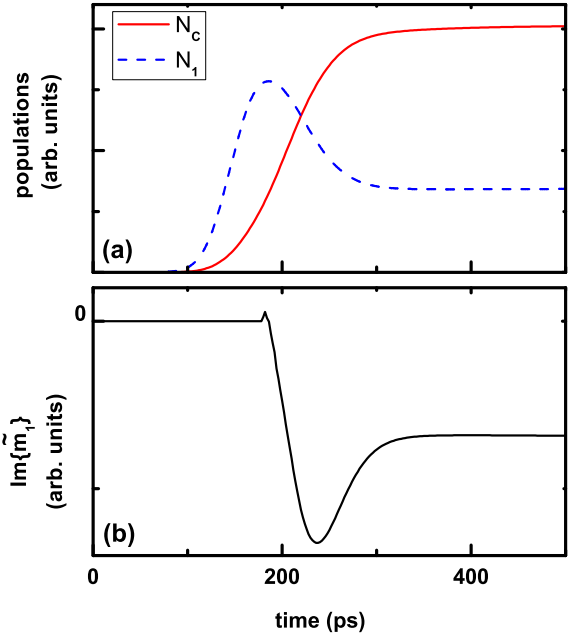


FIG. 2: Time dependent results for the populations of the condensate state N_c and of the first excited state N_1 and for the imaginary part of the coherent scattering amplitude \tilde{m}_1 , for a given value of the excitation pump f above condensation threshold. After an initial transient, all the quantities reach a stationary value.

Fig. 3 (a), we plot the steady-state populations per state, for varying pump intensity. A pump threshold is found at about $f = 12 \text{ ps}^{-1} \mu\text{m}^{-2}$, corresponding to a polariton density $n = N/A \simeq 10 \mu\text{m}^{-2}$ and a total exciton density $n_x \simeq 100 \mu\text{m}^{-2}$ in the incoherent region. Let us remind that the system studied in Ref. 14 is composed by 16 quantum wells. As the polariton modes are expected to have similar amplitudes at all the quantum well positions, in the experimental literature the exciton

density per quantum well is usually estimated by simply dividing the total exciton density by the number of quantum wells^{12,13}. In the present case, following this prescription, the exciton density per quantum well is $7 \mu\text{m}^{-2}$, i.e. two orders of magnitude lower than the exciton saturation density in CdTe $n_{\text{sat}} \simeq 5 \times 10^3 \mu\text{m}^{-2}$. This confirms the validity of our description of polaritons in terms of a weakly interacting Bose field.

Above threshold the condensate population becomes macroscopic. Its growth for increasing f is however suppressed by the corresponding increase of the population of low energy excitations. Consequently, the population distribution cannot be fitted by a Bose-Einstein function. The discrepancy is partly due to the Bogolubov quasiparticle spectrum – characterizing an interacting Bose gas at thermal equilibrium – and partly to quantum fluctuations. In order to distinguish the two contributions, we compare the kinetic result to a distribution computed for an equilibrium interacting Bose gas in the HFB Popov limit,³⁶ accounting for spatial confinement. For this equilibrium distribution, we assume the same density as obtained from the kinetic model for a given pump f , while the temperature is extrapolated from the slope of the high-energy tail of the same kinetic model distribution. In Fig. 3 (a), the result for $f = 50 \text{ ps}^{-1} \mu\text{m}^{-2}$, is compared to the equilibrium HFB Popov distribution with $n = 100 \mu\text{m}^{-2}$ and $T = 20\text{K}$. As expected, the equilibrium result already deviates from the ideal distribution, due to the modified spectrum of the interacting system. However, equilibrium and kinetic results differ significantly in the low-energy region. In particular, the kinetic model predicts a larger condensate depletion. The difference is due to the dominant role played by quantum fluctuations (see also Fig.(4) below), whose amplitude deviates from the equilibrium prediction and has to be evaluated by means of a proper kinetic treatment like the present one. Also in the kinetic model, the energy dispersion is modified by the presence of the condensate because of the two-body interaction, displaying the linear Bogolubov spectrum of collective excitations at low momenta,³⁷ as shown in Fig. 3 (b). Here, the dashed line highlights the linear part of the spectrum. The plot shows that, even at the highest pump intensity, this feature extends over an energy interval smaller than 0.5 meV , well within the measured spectral linewidth.¹⁴ Samples with a significantly smaller polariton linewidth (longer radiative lifetime) would therefore be needed, in order to measure this distinctive feature of BEC. In Fig. 4 we show the values of the coherent scattering rates $v_{k,-k}^{(k)} \text{Im}\{\tilde{m}_k\}$ as a function of the energy of the corresponding states. As expected, they decrease dramatically for increasing energy and their contribution to the dynamics vanishes for states outside the coherent region, thus confirming our initial assumption of separation into two momentum regions. We see also that, for increasing excitation intensity the values of the coherent scattering terms increase, resulting in an increased amplitude of quantum fluctuations.

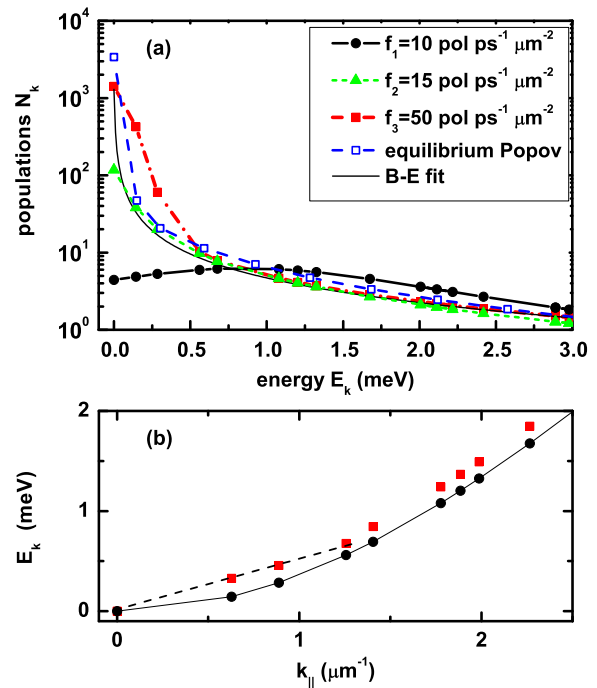


FIG. 3: (a) Steady state populations for increasing pump intensity f . Open squares: equilibrium HFB Popov solution for (n,T) corresponding to the steady-state solution for $f = f_3$. Thin line: B-E distribution fitted to the high-energy tail and to the condensate population for $f = f_3$. (b) Energy dispersion below and above threshold (same legend as above). The dashed line is a guide to the eye to highlight the linear part of the dispersion.

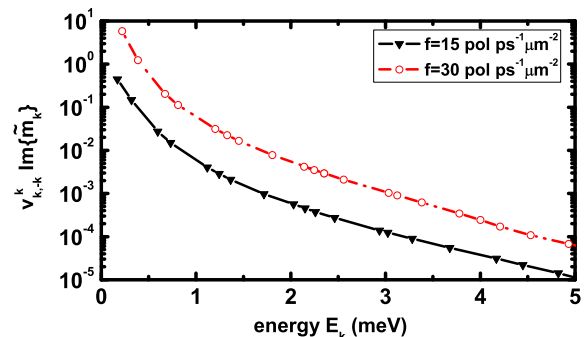


FIG. 4: Coherent scattering contributions $v_{k,-k}^{(k)} \text{Im}\{\tilde{m}_k\}$, for two values of the excitation pump f . The amplitude of such processes decreases dramatically for increasing energy and so their contribution to the dynamics vanishes outside the coherent region.

For increasing system area A , the condensate fraction in the steady-state regime decreases, as shown in Fig. 5 (a), because coherent scattering is favored by a smaller energy gap Δ . Thermal and quantum fluctuations will eventually dominate in the thermodynamic limit of infinite size, resulting in a full condensate depletion, as required by the Hohenberg-Mermin-Wagner

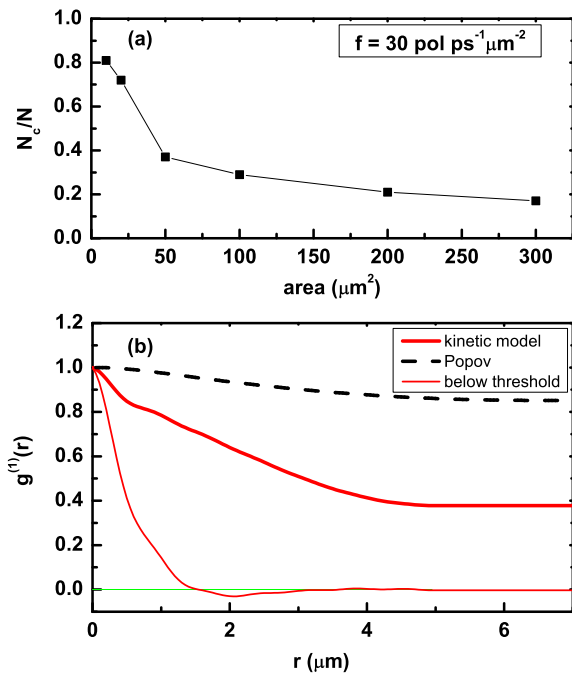


FIG. 5: (a) Condensate fraction as a function of the system area for $f = 30 \text{ ps}^{-1} \mu\text{m}^{-2}$. (b) First order spatial correlation function below and above threshold, compared to the same quantity resulting from the equilibrium HFB Popov model.

theorem. Polariton condensation occurs thanks to the locally discrete nature of the energy spectrum, induced either by artificial confinement or by disorder. In a realistic system^{13,17,35}, localization could therefore affect the polariton BEC, independently of other parameters like Rabi splitting and exciton saturation density.

We finally study the influence of quantum fluctuations on the one-body spatial correlation $g^{(1)}(\mathbf{r}, \mathbf{r}') = n(\mathbf{r}, \mathbf{r}')/\sqrt{n(\mathbf{r})n(\mathbf{r}')}$. The one-body density matrix $n(\mathbf{r}, \mathbf{r}')$ is the direct expression of ODLRO that characterizes BEC.^{2,3} It depends on $|\mathbf{r} - \mathbf{r}'|$ for a uniform system and can be computed in terms of the Fourier transform of the population N_k . The density in the denominator renormalize the shape of the condensate wave function, hence we expect the averaged quantity $g^{(1)}(\mathbf{r}) \equiv 1/A \int d\mathbf{R} g^{(1)}(\mathbf{R}, \mathbf{R} + \mathbf{r})$ to be scarcely affected by the assumption of a uniform condensate. In Fig. 5 (b), we plot $g^{(1)}(\mathbf{r})$ below and above the condensation threshold. Below threshold, correlations vanish for distances larger than $1 - 2 \mu\text{m}$, as predicted by both the kinetic model and the equilibrium HFB Popov approach. Above threshold, the correlation length increases and $g^{(1)}(r)$ remains finite over the whole system size. However, for all values of the pump, $g^{(1)}(r)$ remains smaller than 0.5 at distances larger than $5 \mu\text{m}$, whereas the equilibrium HFB Popov result is significantly larger, due to a larger condensate fraction. Therefore the effect of quantum fluctuations turns out to strongly affect the formation of ODLRO. The quantity $g^{(1)}(r)$ could be easily accessed

in an experiment in which the light emitted by different positions on the sample is made interfere. For such an experiment, we therefore predict the increase of the spatial correlation length as a signature of condensation, with a correlation staying below 0.5 because of quantum fluctuations, even far above the threshold.

Finally, we mention that we have also performed simulations for material parameters modeling a GaAs microcavity with Rabi splitting $2\hbar\Omega_R = 7 \text{ meV}$, detuning $\delta = 0 \text{ meV}$, lattice temperature $T = 10 \text{ K}$, and system area $A = 100 \mu\text{m}^2$. In this case $v_{XX} = 6 \times 10^{-5} \text{ meV}$, $v_{sat} = -0.15 \times 10^{-5} \text{ meV}$ and the resulting polariton-polariton interaction matrix element at zero momentum is $v_{0,0}^{(0)} = 1.5 \times 10^{-5} \text{ meV}$. For this case as well, we observe the occurrence of polariton condensation and the partial suppression of the ODLRO (not shown). Quantitatively, we notice that in this case the total exciton density at threshold is $n_x \simeq 500 \mu\text{m}^{-2}$, significantly higher than in the previous case. Nevertheless, as the number of quantum wells needed to achieve 7 meV Rabi splitting is at least 4, the estimated exciton density per quantum well is about $100 \mu\text{m}^{-2}$, namely still one order of magnitude lower than the saturation density for GaAs, $n_{sat} = 2 \times 10^3 \mu\text{m}^{-2}$.²⁸ Our approach is thus justified also in this case.

IV. CONCLUSIONS

In conclusion, the present model shows that the dynamics of quantum fluctuations significantly affects polariton BEC and the formation of ODLRO in a polariton condensate. In a typical case, quantum fluctuations partially deplete the condensate, already slightly above threshold. Quantitatively, the effect depends on the locally discrete energy spectrum, due to trapping or to disorder. We predict that the observation of BEC and ODLRO should be favored by smaller polariton size, as in the recently studied polariton “quantum boxes”,³⁵ or in local minima of the disorder potential. This suggests that, for a given sample, a study of the polariton localization length in the lowest energy states¹⁷ could give deeper insight into the BEC mechanism.

Acknowledgments

We are grateful to I. Carusotto and R. Zimmermann for fruitful discussions. We acknowledge financial support from the Swiss National Foundation through project N. PP002-110640.

APPENDIX

Equations (8) are derived under the assumption that 3-body and higher order correlation terms can be factored. In this Appendix we provide some detail on their

derivation. Equations for the populations N_c and \tilde{N}_k , with respect to the polariton-polariton interaction part, result directly from Heisenberg time-evolution of operators. The corresponding exciton-phonon term $\dot{N}|_{ph}$ is obtained within a standard Boltzmann kinetics in the Markov limit,⁹ while for the exciton-exciton term $\dot{N}|_{XX}$ we have used the equations introduced by Porrás *et al.* in Ref. 22. Some less straightforward steps were taken to obtain the equations describing the scattering amplitudes \tilde{m}_k . First, as pointed out in the text, we included only the dynamics induced by polariton-polariton scattering Hamiltonian within the coherent region. Then, Heisenberg equations of motion result in the following equations

$$\begin{aligned}
i\hbar\dot{\tilde{m}}_k &= 2(\hbar\omega_k - v_{k,0}^{(0)})\tilde{m}_k + v_{k,0}^{(0)}\langle\hat{a}^\dagger\hat{a}^\dagger(\hat{a}^\dagger\hat{a} + \hat{a}\hat{a}^\dagger)\tilde{p}_k\tilde{p}_{-k}\rangle \\
&- 4\sum_q v_{k,0}^{(0)}\langle\hat{a}^\dagger\hat{a}^\dagger\tilde{p}_q^\dagger\tilde{p}_q\tilde{p}_k\tilde{p}_{-k}\rangle \\
&+ v_{k,-k}^{(k)}\langle\hat{a}^\dagger\hat{a}^\dagger\hat{a}\hat{a}(\tilde{p}_{-k}^\dagger\tilde{p}_{-k} + \tilde{p}_k\tilde{p}_k^\dagger)\rangle \\
&+ \sum_{qq'} v_{q,q'}^{(k-q)}\langle\hat{a}^\dagger\hat{a}^\dagger(\tilde{p}_{q+q'-k}^\dagger\tilde{p}_{-k} + \tilde{p}_k\tilde{p}_{q+q'+k}^\dagger)\tilde{p}_q\tilde{p}_{q'}\rangle \\
&- \sum_q v_{q,-q}^{(q)}\langle(\hat{a}\hat{a}^\dagger + \hat{a}^\dagger\hat{a})\tilde{p}_q^\dagger\tilde{p}_{-q}^\dagger\tilde{p}_k\tilde{p}_{-k}\rangle. \quad (\text{A.1})
\end{aligned}$$

Then, by neglecting 3-body correlations, we can introduce the following factorizations:

$$\langle\hat{a}^\dagger\hat{a}^\dagger\hat{a}^\dagger\tilde{a}\tilde{p}_k\tilde{p}_{-k}\rangle \simeq (N_c - 2)\tilde{m}_k; \quad (\text{A.2})$$

$$\begin{aligned}
\langle\hat{a}^\dagger\hat{a}^\dagger\tilde{p}_q^\dagger\tilde{p}_q\tilde{p}_k\tilde{p}_{-k}\rangle &\simeq (\tilde{N}_q - \delta_{q,k}\tilde{N}_k - \delta_{q,-k}\tilde{N}_{-k})\tilde{m}_k \\
&+ \tilde{N}_{q,k}\tilde{m}_{q,-k} + \tilde{N}_{q,-k}\tilde{m}_{q,k}; \quad (\text{A.3})
\end{aligned}$$

$$\langle\hat{a}^\dagger\hat{a}\tilde{p}_q^\dagger\tilde{p}_{-q}^\dagger\tilde{p}_k\tilde{p}_{-k}\rangle \simeq N_c\langle\tilde{p}_q^\dagger\tilde{p}_{-q}^\dagger\tilde{p}_k\tilde{p}_{-k}\rangle; \quad (\text{A.4})$$

$$\langle\hat{a}^\dagger\hat{a}^\dagger\hat{a}\tilde{a}\tilde{p}_k\tilde{p}_k\rangle \simeq N_c(N_c - 1)\tilde{N}_k; \quad (\text{A.5})$$

$$\begin{aligned}
\langle\hat{a}^\dagger\hat{a}^\dagger\tilde{p}_{q+q'-k}^\dagger\tilde{p}_{-k}\tilde{p}_q\tilde{p}_{q'}\rangle &\simeq 2\tilde{N}_{q+q'-k,q'}\tilde{m}_{q,-k} \\
&+ \tilde{N}_{q+q'-k,-k}\tilde{m}_{q,q'} \\
&- \delta_{q,k}\delta_{q',k}\tilde{N}_k\tilde{m}_k. \quad (\text{A.6})
\end{aligned}$$

From here, within the assumption of a spatially homogeneous system, some of the momentum sums can be carried out explicitly and Eq.(8) is finally obtained.

We now turn to the evaluation of the two-body correlations $\langle\tilde{p}_q^\dagger\tilde{p}_{-q}^\dagger\tilde{p}_k\tilde{p}_{-k}\rangle$. As explained in the text, they are evaluated in a quasi-stationary limit, via the stationary solution of the Bogolubov problem. In terms of collective excitation operators $\hat{\Lambda}_k$, defined in Eq. (7), this quantity is rewritten as:

$$\begin{aligned}
\langle\tilde{p}_q^\dagger\tilde{p}_{-q}^\dagger\tilde{p}_k\tilde{p}_{-k}\rangle &\simeq \frac{\langle\hat{a}\hat{a}^\dagger\hat{a}^\dagger\tilde{p}_q^\dagger\tilde{p}_{-q}^\dagger\tilde{p}_k\tilde{p}_{-k}\rangle}{(N_c + 1)(N_c + 2)} \quad (\text{A.7}) \\
&= \frac{N^2}{(N_c + 1)(N_c + 2)}\langle\hat{\Lambda}_q^\dagger\hat{\Lambda}_{-q}^\dagger\hat{\Lambda}_k\hat{\Lambda}_{-k}\rangle.
\end{aligned}$$

The correlation amplitude for the field $\hat{\Lambda}_k$ is then computed by using the Bogolubov transformation $\hat{\Lambda}_k = U_k\hat{\alpha}_k + V_k^*\hat{\alpha}_{-k}^\dagger$. All the resulting terms are factored as products of the Bogolubov quasi-particle populations $\bar{N}_k = \langle\hat{\alpha}_k^\dagger\hat{\alpha}_k\rangle$, as:

$$\langle\hat{\alpha}_k^\dagger\hat{\alpha}_q^\dagger\hat{\alpha}_k\hat{\alpha}_q\rangle \simeq \bar{N}_k(\bar{N}_q - \delta_{kq}). \quad (\text{A.8})$$

Collecting all the terms, we finally recover Eq.(10). In this equation, single-particle and quasi-particle populations are related with each other through the expression

$$\langle\tilde{p}_k^\dagger\tilde{p}_k\rangle \simeq \frac{N}{N_c + 1}[(|U_k|^2 + |V_k|^2)\bar{N}_k + |V_k|^2]. \quad (\text{A.9})$$

* davide.sarchi@epfl.ch

¹ D. Pines and P. Nozieres, *The theory of quantum liquids* Vols. 1 and 2 (Addison-Wesley, Redwood City, 1966).

² I. Bloch, T. W. Hänsch, T. Esslinger, *Nature* **403**, 166 (2000).

³ O. Penrose and L. Onsager, *Phys. Rev.* **104**, 576 (1956).

⁴ L. Pitaevskii and S. Stringari, *Bose-Einstein condensation* (Oxford University Press, 2003).

⁵ A. Griffin, D. W. Snoke, and S. Stringari, *Bose-Einstein condensation* (Cambridge Univ. Press, Cambridge, 1995).

⁶ D. Snoke, *Science* **298**, 1368 (2002).

⁷ F. M. Marchetti, J. Keeling, M. H. Szymanska and P. B. Littlewood, *Phys. Rev. Lett.* **96**, 066405 (2006).

⁸ F. P. Laussy, G. Malpuech, A. Kavokin and P. Bigenwald, *Phys. Rev. Lett.* **93**, 016402 (2004).

⁹ T. D. Doan, H. T. Cao, D. B. Tran Thoai and H. Haug,

Phys. Rev. B **72**, 085301 (2005).

¹⁰ P. Schwendimann and A. Quattropani, *Phys. Rev. B* **74**, 045324 (2006).

¹¹ H. Deng, G. Weihs, C. Santori, J. Bloch and Y. Yamamoto, *Science* **298**, 199 (2002).

¹² H. Deng, G. Weihs, D. Snoke, J. Bloch and Y. Yamamoto, *PNAS* **100**, 15318 (2003).

¹³ M. Richard, J. Kasprzak, R. Andr, R. Romestain and Le Si Dang, *Phys. Rev. B* **72**, 201301(R) (2005).

¹⁴ J. Kasprzak, M. Richard, S. Kundermann, A. Baas *et al.*, *Nature*, 443, 409 (2006).

¹⁵ I. V. Belousov and V. V. Frolov, *Phys. Rev. B* **54**, 2523 (1996).

¹⁶ P. C. Hohenberg, *Phys. Rev.*, **158**, 383 (1967).

¹⁷ W. Langbein and J. M. Hvam, *Phys. Rev. Lett.* **88**, 47401 (2002).

- ¹⁸ J. Lauwers, A. Verbeure, and V. A. Zagrebnov, *J. Phys. A* **36**, L169 (2003).
- ¹⁹ O. Lenoble, L. A. Pastur and V. A. Zagrebnov, *C. R. de Physique* **5**, 129 (2004).
- ²⁰ Y. Castin and R. Dum, *Phys. Rev. A* **57**, 3008 (1998).
- ²¹ C. W. Gardiner and P. Zoller, *Phys. Rev. A* **58**, 536 (1998).
- ²² D. Porras, C. Ciuti, J. J. Baumberg and C. Tejedor, *Phys. Rev. B* **66**, 085304 (2002).
- ²³ The restriction to the lower polariton branch implies the approximation of structureless polaritons. We assume that the Rabi splitting and the Hopfield factors do not change within the range of densities considered. This assumption was checked evaluating the density-renormalized Rabi splitting $\tilde{\Omega}_R = \Omega_R(1 - N_{exc}/N_{sat})$.²⁴
- ²⁴ C. Ciuti, P. Schwendimann and A. Quattropani, *Semicond. Sci. Technol.* **18**, S279 (2003).
- ²⁵ G. Rochat, C. Ciuti, V. Savona, C. Piermarocchi *et al.*, *Phys. Rev. B* **61**, 13856 (2000).
- ²⁶ S. Ben-Tabou de-Leon and B. Laikhtman, *Phys. Rev. B* **63**, 125306 (2001).
- ²⁷ S. Okumura and T. Ogawa, *Phys. Rev. B* **65**, 035105 (2002).
- ²⁸ S. Schmitt-Rink, D. S. Chemla and D. A. B. Miller, *Phys. Rev. B* **32**, 6601 (1985).
- ²⁹ F. Tassone, C. Piermarocchi, V. Savona, A. Quattropani and P. Schwendimann, *Phys. Rev. B* **56**, 7554 (1997).
- ³⁰ C. Piermarocchi, F. Tassone, V. Savona, A. Quattropani and P. Schwendimann, *Phys. Rev. B* **53**, 15834 (1996).
- ³¹ C. W. Gardiner, M. D. Lee, R. J. Ballagh, M. J. Davis and P. Zoller, *Phys. Rev. Lett.* **81**, 5266 (1998).
- ³² R. J. Dodd, M. Edwards, C. W. Clark and K. Burnett, *Phys. Rev. A* **57**, R32 (1998).
- ³³ Xia-Ji Liu, Hui Hu, A. Minguzzi and M. P. Tosi, *Phys. Rev. A* **69**, 043605 (2004).
- ³⁴ A. J. Leggett, *Rev. Mod. Phys.* **73**, 307 (2001).
- ³⁵ O. El Daif, A. Baas, T. Guillet, J.-P. Brantut *et al.*, *Appl. Phys. Lett.* **88**, 061105 (2006).
- ³⁶ A. Griffin, *Phys. Rev. B* **53**, 9341 (1996).
- ³⁷ J. Steinhauer, R. Ozeri, N. Katz and N. Davidson, *Phys. Rev. Lett.* **88**, 120407 (2002).